Low-Complexity Energy-Efficient Resource Allocation for Delay-Tolerant Two-Way OFDM Relays

Tiantian Yu[1], Yanliang Jin[1], Weisi Guo[2], Changli Fang[1], Wei Deng[1], and Tao Wang[1], *Senior Member, IEEE*

[1]School of Communication & Information Engineering, Shanghai University, China. [2]School of Engineering, University of Warwick, UK. Corresponding author e-mail: yutianyoujian@163.com.

***Abstract*—Energy-efficient wireless communication is becoming increasingly important, especially for wireless devices with a limited battery life and cannot be recharged on a frequent basis. In this paper, a bit allocation algorithm to minimize the total energy consumption for transmitting a bit successfully is proposed for a two-way orthogonal frequency-division multiplexing (OFDM) relay system, whilst considering the constraints of quality-of-service (QoS) and total transmit power. Our scenario is fit for the delay-tolerant services delivered through low-complexity devices in application areas of IoT and M2M communications. Unlike existing bit allocation schemes, which maximize the energy efficiency by measuring "bits-per-Joule" with fixed bidirectional total bit rates constraint and no power limitation, our scheme adapts the bidirectional total bit rates and their allocation on each subcarrier with a total transmit power constraint.**

In order to do so, we propose a new idea to decompose the optimization problem. The problem is solved in two general steps. The first step allocates the bit rates on each subcarrier when the total bit rate of each user is fixed. In the second step, the Lagrangian multipliers are used as the optimization variants, and the dimension of the variant optimization is reduced from 2N to 2, where N is the number of subcarriers. We also prove that the optimal point is on the bounds of the feasible region, thus the optimal solution could be searched through the bounds. The dimension of the variant optimization can be further reduced to 1 by variant substitution when searching through each bound, which significantly reduces the complexity of the proposed algorithm. Simulations are conducted to evaluate the transmit energy efficiency (EE) and spectral efficiency (SE), which demonstrate an average improvement of EE of about 200% over the current non-optimized systems.

***Index Terms*—Energy efficiency, bit allocation, two-way relay, orthogonal frequency-division multiplexing (OFDM), low complexity, machine-to-machine (M2)**

I. INTRODUCTION

Increasing demand for wireless capacity growth in the past several years has led to growing research in energy efficiency and sustainability. For small devices and sensors, which make up the bulk of the 6 billion connected Internet-of-Things (IoT), the mains supply is typically not available and their battery cannot be easily replaced or recharged on a frequent basis [1]. It is likely that these low powered IoT devices will communicate via relays to a local hub, and the Energy efficiency (EE) becomes an important metric. EE can be evaluated by the total energy consumption per successfully received message (Joules-per-bit). In general, research is typically focused on minimizing the joule per bit [2], [3], or maximizing bits-per-Joule [4], [5]. However, there is greater opportunity in IoT devices to improve energy efficiency than in cellular radio, due to the delay-tolerant nature of the data. Yet, the devices are relatively simple and cannot perform complex signal processing algorithms. Therefore, the EE optimization algorithms developed need to be low complexity.

In orthogonal frequency-division multiplexing (OFDM), frequency selective fading can be effectively combated and high spectral efficiency can be achieved. This is why OFDM serves as an essential technique in the current and next generation mobile communications. Multiple relay-based OFDM systems have been proposed under LTE-A and IEEE 802.16 due to its potential to enhance throughput and extend coverage [6]. A number of important relay protocols have already been proposed in the past decade, such as the amplify-and-forward (AF) and decode-and-forward (DF) protocols [7]-[10]. Since the development of physical-layer network coding [11], research has gone to investigate this topic further [12]-[15] to show system throughput improvements of over 100%. Therefore, in this paper, we will investigate a two-way relay OFDM system using the AF protocol. Previous work has largely focused on the optimization for spectral efficiency (SE) [16-18], however, the optimal point of SE is not necessarily equivalent to that of EE [19], so the optimization of EE under different scenarios is another significant problem we should consider. In the past, EE optimization of direct links was analyzed in [4] and [20]. In [4], the EE is optimized in frequency-selective channels using multi-carriers, where the constraints of sum rate and total power consumption including circuit power were considered. In [20], the downlink and uplink of orthogonal frequency-division multiplexing access (OFDMA) networks with QoS and fairness issues were considered. Yet, we know that the methods that allocate resources to optimize EE in direct links are not the same as those relay based links. The reason lies in the differences of system models and the types of resource available to allocate. Whilst SE and EE optimization for relay deployment has been examined recently [21], limited work has been done to address EE optimization for relay based communication on the radio resource allocation level (see [5] for one/two-way relaying in OFDM systems).

For real time services [23], existing work in [5, 22] have analyzed the optimal EE is acquired under the QoS and symbol error rate with multiple relays. Real-time services [23] constrains a sum rate for individual users, which is not required in delay tolerant services, where only minimum rate requirements are needed for each user. Due to the fixed bidirectional total bit rates constraints, the methods of [5] and [22] to allocate resources are not suitable in delay-tolerant services. Another problem in [5] and [22] is that transmit power consumption is not limited, which makes it hard to use those corresponding methods in low power situations. Other related work includes [24-26], but none of them have considered QoS requirements.

In our paper, we consider the QoS requirements in the form of delay-tolerant data demand and total power restrictions, which to the best of our knowledge has not been considered before. In order to reduce the complexity of the algorithm, we introduce a new idea to reduce the dimension of the variants, which resolves the optimization problem in two steps and is achieved by looking at the Lagrangian multipliers as the optimization variants. To the best of our knowledge, this also hasn't been studied before. The rest of the paper is organized as follows. In Section II, a two-way OFDM relay system model is presented. In Section III, the EE optimization problem is formulated. The low-complexity algorithm for resource allocation is proposed in section IV. In section V, simulation results are provided and analyzed. Finally, we conclude the paper in section VI.

II. SYSTEM MODEL

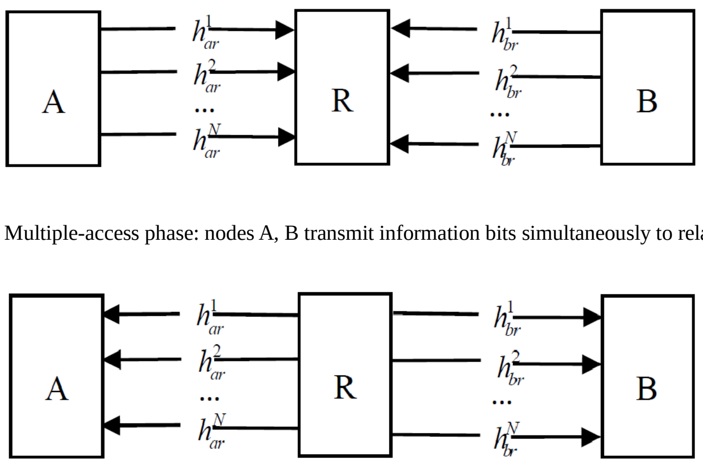

(a) Multiple-access phase: nodes A, B transmit information bits simultaneously to relay R.

(b) Broadcast phase: relay R broadcasts the processed information to nodes A and B.

Fig.1. Multiple access and broadcast process, the total duration time is 2T, and channel reciprocity is assumed.

We consider a two-way OFDM relay system consisting of three nodes. The two source nodes A and B exchange information bi-directionally with N subcarriers through the AF relay R. Each node is equipped with a single antenna, and the system works at the half-duplex mode. Assume the signal between two source nodes is severely attenuated, therefore, the direct link is not considered. The transmission process is composed of two phases: a multiple-access (MA) phase and a broadcast (BC) phase, as illustrated in Fig.1. The time duration of the two phases is the same, donated as T. In the MA phase, nodes A and B simultaneously transmit information bits to the relay node R. The two signals along with the noise are superimposed first, and then amplified in relay R. In the BC phase, relay R broadcasts the processed signal to the nodes A and B.

Whilst the majority of papers assume that the channel state information (CSI) is perfect, we know that in practice, the CSI is not perfect, which makes it hard to find an explicit expression of the system EE. As shown in Fig.1, the channel coefficients of MA and BC phases are the same, which is true when the system works at the time division duplex (TDD) mode, where channel reciprocity applies. The channel is considered to be block fading, and the channel coefficients are constant during the time duration 2T, meaning the channel gain is constant during one complete communication cycle.

The total operational energy consumption consists of two parts: transmit power consumption (radio-head) and circuit power consumption (over-head) [27]. We ignore the overhead circuit power consumption, due to the fact that it scales in complex ways with data throughput, and the complexity is dependent on specific hardware technologies that we wish to avoid becoming sensitive to. We want to focus on the bit error rate and its direct relationship to the transmit power of the signal. Based on the consideration, we will omit the circuit power consumption. Therefore, the EE can be expressed as

$$\eta_{EE} = \frac{P_T}{(B_{ab}+B_{ba})/2T} = \frac{2TP_T}{B_{ab}+B_{ba}}, \tag{1}$$

where T is the duration of one phase (MA or BC), the factor of 2 is due to the half-duplex bidirectional communication. P_T is the overall transmit power consumption. B_{ab} and B_{ba} are respectively the sum message bits transmitted in $A \to B$ direction and $B \to A$ direction in one complete transmission. Note that the denominator of the first fraction in (1) represents the sum rate of the system. Suppose nodes A and B respectively transmit B_{ab}^i and B_{ba}^i bits at the same time on the ith subcarrier to relay R, and then relay R broadcasts its processed information to the two source nodes, thus B_{ab} and B_{ba} can be formulated as:

$$B_{ab} = \sum_{i=1}^{N} B_{ab}^{i}, \tag{2a}$$

$$B_{ba} = \sum_{i=1}^{N} B_{ba}^{i}. \tag{2b}$$

Many OFDM systems fix T as a constant, and we conform to this setting. We should nevertheless point out that T can also be taken as an optimization variant [29], which leads to a better performance system. The approximate minimum total transmit power of the three nodes on the ith subcarrier can be derived as [5], [29]:

$$\begin{aligned} P_{t_i} &= (P_a^{t_i} + P_b^{t_i} + P_r^{t_i})_{\min} \\ &\approx \frac{N_0(2^{\frac{B_{ab}^i}{TW/N}} - 1)}{2\,|h_{eff}^i|^2} + \frac{N_0(2^{\frac{B_{ba}^i}{TW/N}} - 1)}{2\,|h_{eff}^i|^2}, \end{aligned} \tag{3}$$

where $|h_{eff}^i| \triangleq 1/(\frac{1}{|h_{ar}^i|} + \frac{1}{|h_{br}^i|})$ ($A \triangleq B$ means that A is defined as B) can be viewed as an effective channel gain on the ith subcarrier between the two source nodes due to the usage of the relay, W is the bandwidth of nodes A and B . The approximate expression of (3) comes from the approximation

$$2^{\frac{B_{ab}^i}{TW/N}} - 1 \approx 2^{\frac{B_{ab}^i}{TW/N}}. \tag{4}$$

The approximation above is relatively accurate in high SE region (i.e. $B_{ab}^i / (TW)$ is large), which is nearly established in low SE region when N is not too small. With the approximation, we can simplify the derivation process, so (3) is used in this paper to calculate the transmit power. The overall transmit power P_T therefore can be expressed as

$$\begin{aligned} P_T(\mathbf{B}_{ab}, \mathbf{B}_{ba}) &= \sum_{i=1}^{N} P_{t_i} \\ &\approx \sum_{i=1}^{N} \frac{N_0(2^{\frac{B_{ab}^i}{TW/N}} - 1)}{2\,|h_{eff}^i|^2} + \sum_{i=1}^{N} \frac{N_0(2^{\frac{B_{ba}^i}{TW/N}} - 1)}{2\,|h_{eff}^i|^2}. \end{aligned} \tag{5}$$

Furthermore, by substituting equations (2a), (2b), and (5) into equation (1), we can get the expression of EE.

III. PROBLEM FORMULATION

The objective of the paper is to minimize the EE of the system under two restrictions: first, the respective throughputs of node A and B; second, the total power consumption of the system. The first constraint can guarantee a satisfactory measure of bit rates for each user, and the second constraint ensures that the total energy consumption is confined to the acceptable level.

Problem 1: It is shown from above that the EE can be finally expressed as the function of B_{ab}^i and B_{ba}^i, thus we can optimize the EE by bit allocation.

Let $\mathbf{B_{ab}} = \left\{B_{ab}^1, B_{ab}^2, \cdots, B_{ab}^N\right\}^T$ and $\mathbf{B_{ba}} = \left\{B_{ba}^1, B_{ba}^2, \cdots, B_{ba}^N\right\}^T$ respectively denote the bit sets of nodes A and B, $\mathbf{1}$ denotes the all-one vector of size $N \times 1$, then the problem can be formulated as

$$\min_{\mathbf{B}_{ab},\mathbf{B}_{ba}} \quad \eta_{EE} = \frac{P_T(\mathbf{B}_{ab},\mathbf{B}_{ba})}{(\mathbf{1}^T\mathbf{B}_{ab}+\mathbf{1}^T\mathbf{B}_{ba})/2T} = \frac{2TP_T(\mathbf{B}_{ab},\mathbf{B}_{ba})}{\mathbf{1}^T\mathbf{B}_{ab}+\mathbf{1}^T\mathbf{B}_{ba}}, \tag{6}$$

$$s.t. \quad \mathbf{1}^T\mathbf{B}_{ab} \geq \Gamma_{ab}, \tag{6a}$$

$$\mathbf{1}^T\mathbf{B}_{ba} \geq \Gamma_{ba}, \tag{6b}$$

$$P_T(\mathbf{B}_{ab},\mathbf{B}_{ba}) \leq P_{max}, \tag{6c}$$

$$\mathbf{B}_{ab} \succ \mathbf{0}, \tag{6d}$$

$$\mathbf{B}_{ba} \succ \mathbf{0}. \tag{6e}$$

We should point out that our conditions of (6d) and (6e) are different from those of the previous papers [2], [5], where B_{ab}^i and B_{ba}^i can be zero. The two constraints are reasonable in situations where the QoS requirements of the source nodes are relatively high that all the sub-channels should be used to transmit the information bits. In fact, (6d) and (6e) establish when Γ_{ab} and Γ_{ba} satisfy the constraints

$$\Gamma_{ab} > \kappa, \tag{7a}$$

$$\Gamma_{ba} > \kappa. \tag{7b}$$

Later we will prove the constraints above and obtain the value of κ .

We should note that the constraints for $\mathbf{1}^T\mathbf{B}_{ab}$ and $\mathbf{1}^T\mathbf{B}_{ba}$ are not necessarily the same, i.e., Γ_{ab} and Γ_{ba} are not definitely equal, because the rate requirements of nodes A and B may be different.

IV. LOW-COMPLEXITY ALGORITHM ANALYSIS

Problem 1 can be solved through two steps. The idea behind this two-step algorithm is that when $\mathbf{1}^T\mathbf{B}_{ab}$ and $\mathbf{1}^T\mathbf{B}_{ba}$ are fixed, i.e., $\sum_{i=1}^{N} B_{ab}^i = B_{ab}$ and $\sum_{i=1}^{N} B_{ba}^i = B_{ba}$, and (6c) does not exist, we can use water-filling method to get the closed-form solution; then we change B_{ab} and B_{ba} (look them as variants), and do some transformation, thereafter, we can make the problem much easier to solve. We will explain our algorithm below.

Problem 2: When $\mathbf{1}^T\mathbf{B}_{ab}$ and $\mathbf{1}^T\mathbf{B}_{ba}$ are fixed, without (6c), (6d) and (6e), problem 1 can be described as

$$\min_{\mathbf{B}_{ab},\mathbf{B}_{ba}} \quad \eta_{EE} = \frac{2TP_T(\mathbf{B}_{ab},\mathbf{B}_{ba})}{\mathbf{1}^T\mathbf{B}_{ab}+\mathbf{1}^T\mathbf{B}_{ba}}, \tag{8}$$

$$s.t. \quad \mathbf{1}^T\mathbf{B}_{ab} = B_{ab}, \tag{8a}$$

$$\mathbf{1}^T\mathbf{B}_{ba} = B_{ba}, \tag{8b}$$

$$B_{ab}^i \geq 0. \tag{8c}$$

Problem 2 can be solved with water-filling algorithm. The water-filling assignment is

$$B_{ab}^i = \max\left(\frac{TW}{N}\log_2\frac{2TW\,|h_{eff}^i|^2}{N_0 N \ln 2}\mu_1, 0\right), \tag{9a}$$

$$B_{ba}^i = \max\left(\frac{TW}{N}\log_2\frac{2TW\,|h_{eff}^i|^2}{N_0 N \ln 2}\mu_2, 0\right), \tag{9b}$$

where μ_1 and μ_2 are the Lagrange multipliers, and can be solved through the constraints (8a) and (8b). In other words, we can get

$$\sum_{i=1}^{N}\max\left(\frac{TW}{N}\log_2\frac{2TW\,|h_{eff}^{i}|^2}{N_0 N\ln 2}\mu_1,0\right)=B_{ab},\tag{10a}$$

$$\sum_{i=1}^{N}\max\left(\frac{TW}{N}\log_2\frac{2TW\,|h_{eff}^{i}|^2}{N_0 N\ln 2}\mu_2,0\right)=B_{ba}.\tag{10b}$$

The full proof can be found in Appendix A.

Assuming the amplitudes of the effective channel gain $|h_{eff}^{i}|\,(i=1,2,\cdots,N)$ are arranged in a descending order, then the values of the elements in $\mathbf{B}_{\mathbf{ab}}$ and $\mathbf{B}_{\mathbf{ba}}$ correspondingly reduce monotonically. Suppose the first L_1 elements in $\mathbf{B}_{\mathbf{ab}}$ and L_2 elements in $\mathbf{B}_{\mathbf{ba}}$ are positive, then (10a) and (10b) can be expressed as:

$$\sum_{i=1}^{L_1}\frac{TW}{N}\log_2\frac{2TW\,|h_{eff}^{i}|^2}{N_0 N\ln 2}\mu_1=B_{ab},\tag{11a}$$

$$\sum_{i=1}^{L_2}\frac{TW}{N}\log_2\frac{2TW\,|h_{eff}^{i}|^2}{N_0 N\ln 2}\mu_2=B_{ba}.\tag{11b}$$

We can see from (11a) that because of the unknown quantity L_1, we cannot obtain the explicit expression of μ_1 on B_{ab}, so is μ_2. Whereas in high speed systems, the requirements of QoS are relatively high, therefore all sub-channels will be used to transmit the message bits, therefore (6d) and (6e) are established. That is to say, $L_1=L_2=N$, which leads to the requirements (12a) and (12b):

$$\mu_1>\frac{N_0 N\ln 2}{2TW\,|h_{eff}|_{\min}^2}=\varsigma,\tag{12a}$$

$$\mu_2>\frac{N_0 N\ln 2}{2TW\,|h_{eff}|_{\min}^2}=\varsigma,\tag{12b}$$

where $|h_{eff}|_{\min}$ is the smallest amplitude in the effective channel gains.

The formulas above are easy to prove. We assume B_{ab_m} and B_{ba_m} are the bit values calculated by $|h_{eff}|_{\min}$ from (9a) and (9b), we conclude that if B_{ab_m} and B_{ba_m} are positive, leading to the constraints (12a) and (12b), then all the elements of $\mathbf{B}_{\mathbf{ab}}$ and $\mathbf{B}_{\mathbf{ba}}$ must be positive. Let $L_1=L_2=N$, from (11a) and (11b), we can derive that

$$B_{ab}=TW\log_2\frac{2TW}{N_0 N\ln 2}(|h_{eff}^{1}\cdots h_{eff}^{N}|^2)^{\frac{1}{N}}\mu_1,\tag{13a}$$

$$B_{ba}=TW\log_2\frac{2TW}{N_0 N\ln 2}(|h_{eff}^{1}\cdots h_{eff}^{N}|^2)^{\frac{1}{N}}\mu_2.\tag{13b}$$

Substituting (12a) and (12b) into (13a) and (13b), we get

$$B_{ab}>TW\log_2\frac{(|h_{eff}^{1}\cdots h_{eff}^{N}|^2)^{\frac{1}{N}}}{|h_{eff}|_{\min}^2}=\kappa,\tag{14a}$$

$$B_{ba}>TW\log_2\frac{(|h_{eff}^{1}\cdots h_{eff}^{N}|^2)^{\frac{1}{N}}}{|h_{eff}|_{\min}^2}=\kappa.\tag{14b}$$

Therefore in high speed systems, from (9a) and (9b), we can get:

$$B_{ab}^{i} = \frac{TW}{N}\log_2 \frac{2TW\,|\,h_{eff}^{i}\,|^2}{N_0 N \ln 2}\mu_1, \qquad (15a)$$

$$B_{ba}^{i} = \frac{TW}{N}\log_2 \frac{2TW\,|\,h_{eff}^{i}\,|^2}{N_0 N \ln 2}\mu_2, \qquad (15b)$$

and by further substituting (15a) and (15b) into (3), we can get P_{t_i}, then we can derive P_T from (5), and finally we obtain the expression of η_{EE} from (1). When $\mathbf{1}^T\mathbf{B}_{ab}$ and $\mathbf{1}^T\mathbf{B}_{ba}$ are fixed, the result is as follows:

$$\eta_{EE} = 2T\frac{\frac{TW}{\ln 2}(\mu_1+\mu_2) - N_0\sum_{i=1}^{N}\frac{1}{|\,h_{eff}^{i}\,|^2}}{B_{ab}+B_{ba}}. \qquad (16)$$

Since μ_1 and B_{ab}, μ_2 and B_{ba} are restricted by (13a) and (13b), we can observe η_{EE} as the function of μ_1 and μ_2.

Based on (14a) and (14b), we can get (7a) and (7b). From the ranges of Γ_{ab} and Γ_{ba}, we can get the ranges of μ_1 and μ_2. According to (13a) and (13b), we can derive

$$\mu_1 \ge \frac{N_0 N \ln 2}{2TW(|\,h_{eff}^{1}\cdots h_{eff}^{N}\,|^2)^{\frac{1}{N}}}2^{\frac{\Gamma_{ab}}{TW}} \triangleq \vartheta_1 \qquad (17a)$$

$$\mu_2 \ge \frac{N_0 N \ln 2}{2TW(|\,h_{eff}^{1}\cdots h_{eff}^{N}\,|^2)^{\frac{1}{N}}}2^{\frac{\Gamma_{ba}}{TW}} \triangleq \vartheta_2 \qquad (17b)$$

Problem 3: We vary μ_1 and μ_2 (equivalent to vary B_{ab} and B_{ba}) in the ranges of (17a) and (17b). Together with the restriction (6c), problem 1 can be transformed to

$$\min_{\mu_1,\mu_2} \quad \eta_{EE} = 2T\frac{\frac{TW}{\ln 2}(\mu_1+\mu_2) - N_0\sum_{i=1}^{N}\frac{1}{|\,h_{eff}^{i}\,|^2}}{B_{ab}+B_{ba}}, \qquad (18)$$

$$s.t. \quad P_T(\mathbf{B}_{ab},\mathbf{B}_{ba}) = \frac{TW}{\ln 2}(\mu_1+\mu_2) - N_0\sum_{i=1}^{N}\frac{1}{|\,h_{eff}^{i}\,|^2} \le P_{max},$$

$$\mu_1 \ge \vartheta_1, \mu_2 \ge \vartheta_2, (13a)\ and\ (13b).$$

We should note that because Γ_{ab} and Γ_{ba} are not definitely equal in Problem 1, the corresponding constraints for μ_1 and μ_2 (equivalent to investigate the values of ϑ_1 and ϑ_2) are not necessarily the same (for the same case, just let $\vartheta_1 = \vartheta_2$). Due to (12a) and (12b), the constraints $\vartheta_1 > \varsigma$ and $\vartheta_2 > \varsigma$ must be established, which are illustrated in Fig. 2. Another point is that since μ_1 and μ_2 are constricted by ϑ_1 and ϑ_2, P_{max} is therefore constricted by the following

$$P_{max} > \frac{TW}{\ln 2}(\vartheta_1+\vartheta_2) - N_0\sum_{i=1}^{N}\frac{1}{|\,h_{eff}^{i}\,|^2} = \rho. \qquad (19)$$

This is easy to understand, since the overall transmit power is an increasing function of the transmission rates, the total transmit power should be larger than the minimum requirement corresponding to the minimum transmission rates. In this paper, we assume (19) is automatically established.

Problem 3 is relatively easy to solve, because it is a two-dimensional optimization problem with a feasible region. The feasible region is plotted in Fig. 2, where $l_1 : \mu_1 = \vartheta_1$, $l_2 : \mu_2 = \vartheta_2$, $l_3 : \frac{TW}{\ln 2}(\mu_1 + \mu_2) - N_0 \sum_{i=1}^{N} \frac{1}{|h_{eff}^i|^2} = P_{max}$. A , B and C are respectively the cross points of the three lines. ϑ_3 and ϑ_4 can be easily calculated by variant substitution. Theorem 1 tells us how to search the optimization solution of problem 3, which is proven in Appendix B.

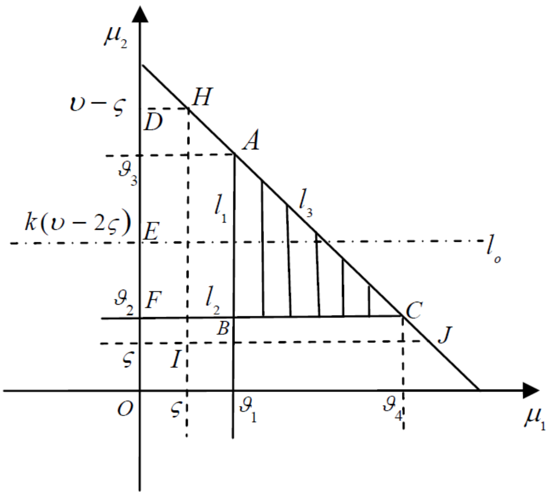

Fig. 2. Feasible region: ΔABC (shadow region).

Theorem 1. The optimal independent variables lie in the bounds of the feasible region.

According to theorem 1, we can get the optimal solution through searching the bounds AB, BC and AC. We fix one of the variants (μ_1 and μ_2) when searching the bounds AB and BC, and substitute one of the variants by another when searching bound AC. Therefore, these searches are just one-dimensional and can be solved efficiently with golden section method. The variant dimension of Problem 1 is 2N, and by using our proposed method, the dimension has been reduced to merely one, so we call our algorithm a reduction-dimension optimization algorithm, which is summarized in algorithm I, where $\mu_i^*, i = 1, 2$ are the optimal solutions of problem 3.

Algorithm I: Proposed reduction-dimension optimization

---

1. Let $\mu_1 \in (\vartheta_1, \vartheta_4)$, $\mu_2 = \vartheta_2$

   Searching the smallest value, donated as η_1 , of (18) through the range of μ_1 by using golden section method. The value of μ_1 corresponding to η_1 is given to r_1 .

2. Let $\mu_1 = \vartheta_1, \mu_2 \in (\vartheta_2, \vartheta_3)$

   Searching the smallest value, donated as η_2 , of (18) through the range of μ_2 by using golden section method. The value of μ_2 corresponding to η_2 is given to r_2 .

3. Let $\mu_1 \in (\vartheta_1, \vartheta_4)$, μ_2 is calculated by the equation of l_3

   Searching the smallest value, donated as η_3 , of (18) through the range of μ_1 by using golden section method section method. The values of μ_1 and μ_2 corresponding to η_3 are respectively given to r_3 and r_4.

4. $\eta = \min(\eta_1, \eta_2, \eta_3)$

   If $\eta = \eta_1$, then $\mu_1^* = r_1, \mu_2^* = \vartheta_2, \eta_{EE}^* = \eta_1$.

   If $\eta = \eta_2$, then $\mu_1^* = \vartheta_1, \mu_2^* = r_2, \eta_{EE}^* = \eta_2$.

   If $\eta = \eta_3$, then $\mu_1^* = r_3, \mu_2^* = r_4, \eta_{EE}^* = \eta_3$.

5. Use (15a) and (15b) to calculate B_{ab}^i and B_{ba}^i, where $\mu_1 = \mu_1^*, \mu_2 = \mu_2^*$.

V. SIMULATION RESULT

In this section, we provide simulation results for the performance of the low-complexity energy-efficient algorithm. The frequency-domain channels are generated using ***N*** i.i.d Rayleigh distributed time-domain taps, where N is the number of subcarriers. The frequency spacing between adjacent subcarriers is 15 kHz. The total time T for one complete transmission is 20ms. We assume that the wireless channels between source nodes and relay node are reciprocal (Fig. 1).

The feasible region is illustrated in Fig. 2. According to the constraints $\vartheta_1 > \varsigma, \vartheta_2 > \varsigma$, and (19), we have

$$P_{max} > \frac{2\varsigma TW}{\ln 2} - N_0 \sum_{i=1}^{N} \frac{1}{|h_{eff}^i|^2} = \rho_1 .$$

Setting $P_{max} = \rho_1 + \vartriangle P$, $\vartheta_1 = \varsigma$, where $\vartriangle P$ is the increment compared to ρ_1. When $\vartriangle P$ is given, l_3 is fixed. Let $\upsilon \triangleq (P_{max} + N_0 \sum_{i=1}^{N} \frac{1}{|h_{eff}^i|^2}) \frac{\ln 2}{TW}$, then we can work out the coordinate of D, as illustrated in Fig. 2. In our simulation, we first fix P_{max}, then vary ϑ_2 (equivalent to change Γ_{ba}) from ς to $\upsilon - \varsigma$ in order to change the feasible region, for example, when l_2 is moved to l_o, point F is moved correspondingly to E. By changing k (showed in Fig. 2) from 0 to 1, we can get different EE and SE. Our simulation result below is based on this method.

Fig. 3 shows the relationship of EE and SE of the proposed algorithm, and we compare this performance through different numbers of subcarriers. Our simulation results show that the EEs under the same SEs change small when the number of subcarriers is larger than 4, so we do not draw them up. Actually ς is changed due to the changing of the number of subcarriers (see (12)), so the EE result will not be the same. The tradeoff of EE and SE is that if we achieve a smaller EE (equal to get a better EE performance), we will get a smaller SE (equal to get a worse SE performance) at the same time, the vice versa. The tradeoff of EE and SE is different when the number of subcarriers is different. When the number of subcarriers is larger than 4, the trends of EE and SE are almost the same with the situation where the number of subcarriers is 4, so their EE and SE tradeoff are almost the same. When the numbers of subcarriers are smaller than 4, the tradeoff are different. For example, compare two situations where the numbers of subcarriers are respectively one and four. From Fig. 3 we can see that when SE is 10bps/Hz, EE in the two situations are almost the same, but when SE is changed to 20bps/Hz, the EE under one subcarrier is almost the half than the EE under four subcarriers, so the performance loss of EE under the four subcarriers is twice than that under the one subcarrier.

Fig. 4 shows the comparison of the optimum EE and the EE calculated through middle point (EE-MP) of l_1. Here we fix P_{max} and vary k to get a different Γ_{ba}. We can see from the results that the performance of EE is improved averagely 200% compared to EE-MP in low Γ_{ba} region. When Γ_{ba} gradually becomes larger, the optimum EE and EE-MP gradually achieve the same value, which is because the feasible region becomes gradually small (l_1 and l_3 are fixed, only l_2 is changed), so the EE results of the two methods approach to each other. Often the feasible region will not be very small, so our optimization algorithm is actually very effective.

Fig. 5 shows the EE results of different numbers of subcarriers. When k is fixed, we change the value of $\triangle P$ to get three group curves. We can see that when $\triangle P$ reduces, EE generally gets larger, which means the performance decreases when P_{max} becomes larger. We can also see that the EE difference becomes smaller in each group when the number of subcarriers increases while the difference between groups becomes larger, for example, the optimum EE of group 1 improves almost 100% compared to group 3 when the number of subcarriers is 5. This is because when the number of subcarriers in each group increases, ς becomes larger, so the feasible region becomes smaller, as the result, the optimum EE and EE-MP gradually close to each other. However, between the groups, the change of $\triangle P$ will affect l_3, changing υ. Because ς is fixed, so $\upsilon - \varsigma$ is changed, thus, when k is fixed, Γ_{ba} is changed, so the feasible region will be determined by the two changed factors: Γ_{ba} and l_3, thus the variation trends between groups are different from those of the same groups when the number of subcarriers increases.

Fig. 6 shows the SE result for different numbers of subcarriers using our optimal method. We change the value of $\triangle P$ to get three group curves. For comparison, we also change the value of k in each group. From the curves we can see that the SE decreases when the number of subcarriers increases, so if we want to get a higher SE, we should reduce the number of subcarriers. Experiment results also show that the change of k can affect SE in some degree, whereas $\triangle P$ can influence SE in large degree. The reason for that is that the change of k can only affect Γ_{ba}, but the change of $\triangle P$ can affect not only Γ_{ba} but also l_3, so the change of $\triangle P$ has a greater influence for feasible region than that of the change of k. If we want to get a higher SE, we should increase $\triangle P$ or increase k, which is useful when we want to improve the overall throughput.

Fig. 7 shows the minimum individual rate assignments in two directions under different numbers of subcarriers. Here the minimum individual rate means the minimum transmit rate among different sub-channels when the number of subcarriers is given. The expressions used for the bidirectional bit assignments are (15a) and (15b). We see that the minimum bit assignments in $A \rightarrow B$ direction is lower than the values in $B \rightarrow A$ direction, which is owe to that the overall throughput in $A \rightarrow B$ direction is larger than that of $B \rightarrow A$ direction. The minimum bit assignment decreases when the number of subcarriers increases, which is because the SE decreases with the number of subcarriers increasing. When the number of subcarriers is fixed, the minimum bit assignment increases when $\triangle P$ becomes larger, which is because the SE increases with the increasing of $\triangle P$.

Fig. 8(a) shows the effective channel gain. Fig. 8(c) shows the bit rate assignments in $A \rightarrow B$ direction and that of $B \rightarrow A$ direction using water-filling method. We also give out the power assignment of each subcarrier in Fig. 8(b). The number of subcarriers used in Fig.8 is 10. From Fig. 8(a) and Fig. 8(c) we can see that the bit rate of individual subcarrier increases when the effective channel gain increases, which is agree with the formula (15a) and (15b), where B_{ab}^i and B_{ba}^i ($i = 1, 2, \cdots, N$) are the increasing functions of $|h_{eff}^i|$. From Fig. 8(b) we can see that the power allocation on individual subcarrier increases with the increasing of effective channel gain, which can be explained by formula (3). From formula (3), we can see that P_{t_i} ($i = 1, 2, \cdots, N$) are determined by B_{ab}^i, B_{ba}^i and $|h_{eff}^i|$. Because B_{ab}^i and B_{ba}^i affect P_{t_i} by exponential form, so they have a greater influence to P_{t_i} than that of $|h_{eff}^i|$. Therefore, the trends of P_{t_i} are the same with that of B_{ab}^i and B_{ba}^i. That is to say, the power allocation on individual subcarrier increases when the effective channel gain increases.

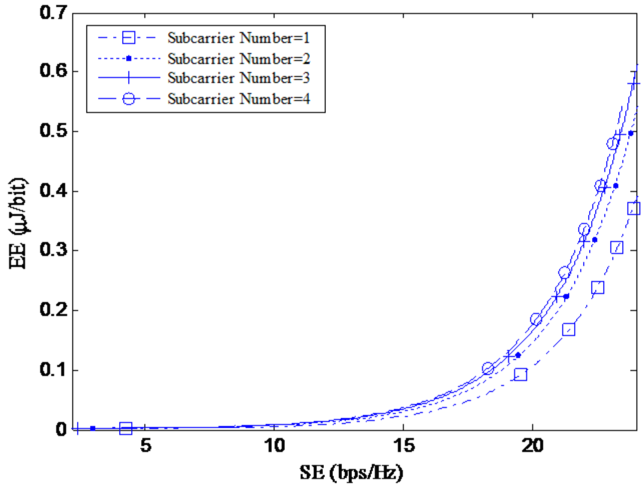

Fig.3. EE verses SE using proposed scheme with the number of subcarriers changed, where $\triangle P = 0.5\text{W}$.

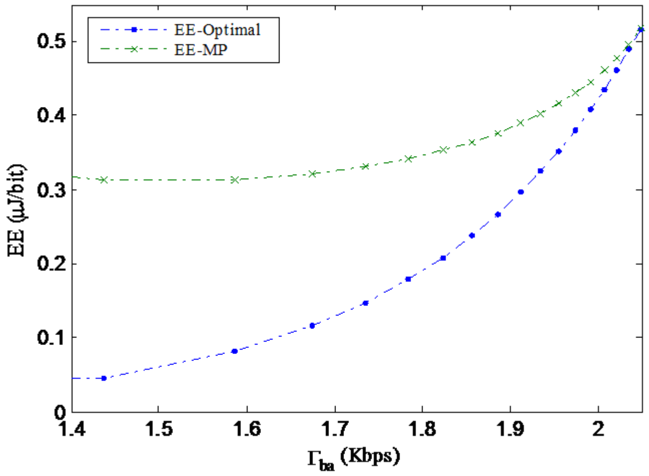

Fig.4. EE verses Γ_{ba} using proposed scheme and EE-MP method, where $\triangle P = 0.5\text{W}$, the number of subcarriers is 4.

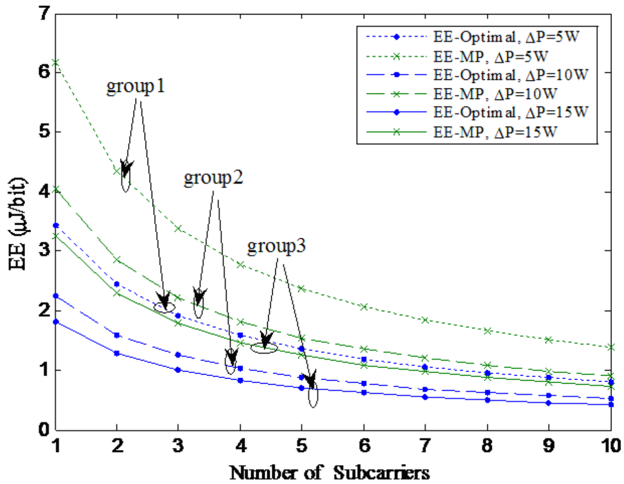

Fig. 5. EE verses number of subcarriers using proposed scheme and EE-MP method with $\triangle P$ changed, where $k = 0.3$.

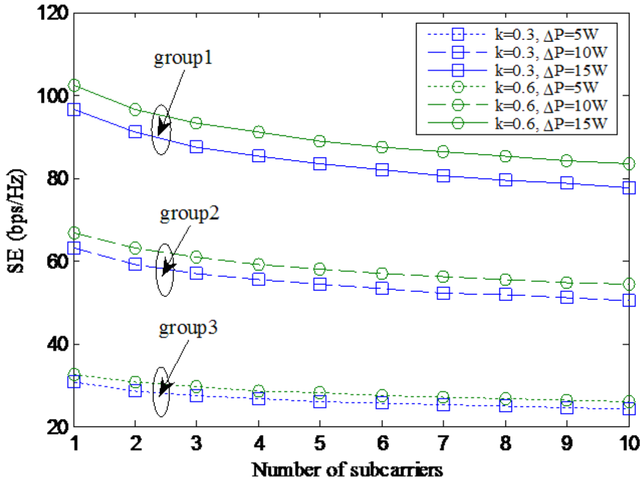

Fig. 6. SE verses number of subcarriers using proposed scheme and EE-MP method with k and $\triangle P$ changed.

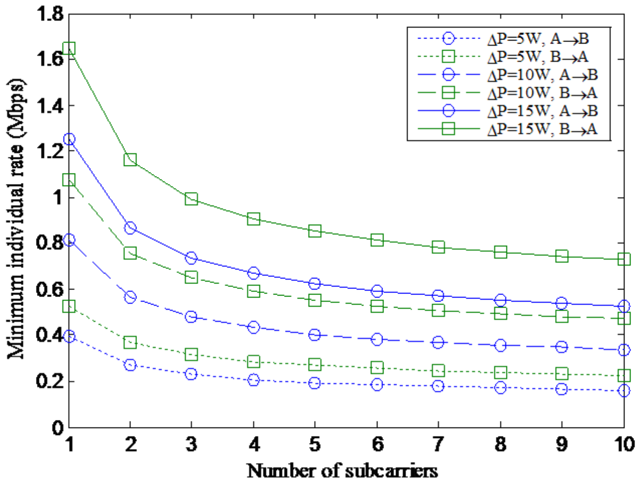

Fig. 7. Bi-directional minimum individual rate verses number of subcarriers with $\triangle P$ changed.

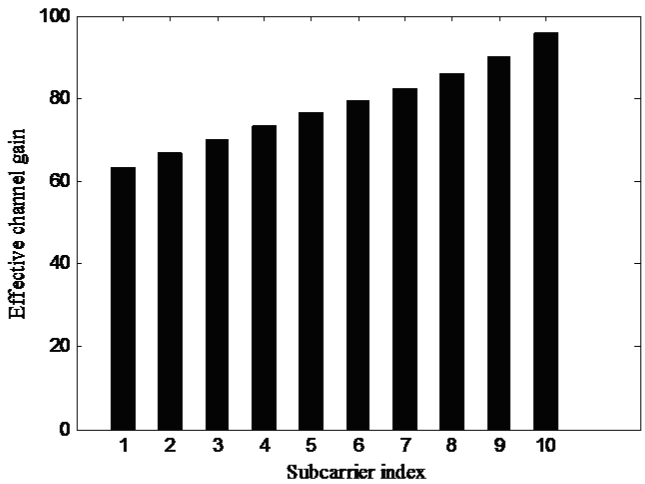

(a) Effective channel gain of sub-channel.

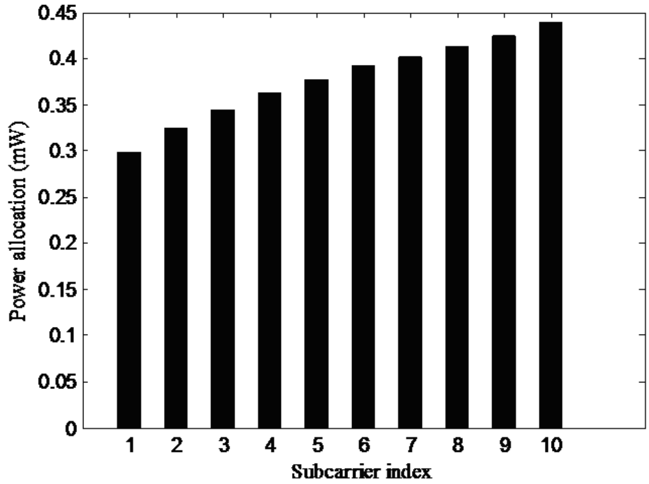

(b) Power allocation on individual subcarrier.

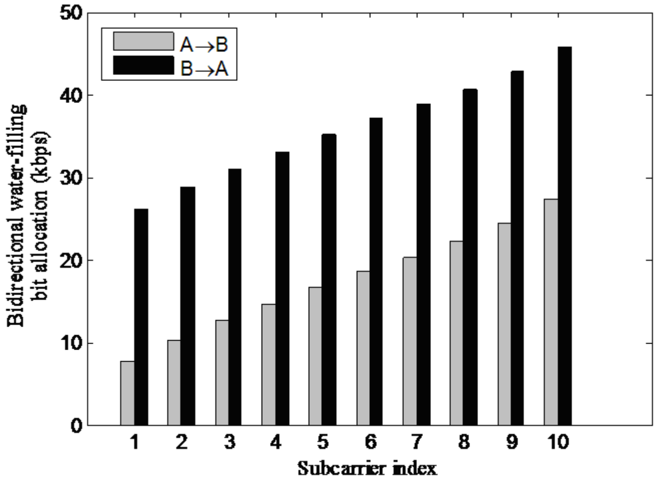

(c) Bidirectional bit allocation on individual subcarrier.

Fig. 8. Channel conditions and the corresponding assignments of power and bit on each subcarrier, where the number of subcarriers is 10, $\triangle P = 0.5\text{W}$, $\vartheta_1 = \varsigma$, $\vartheta_2 = 3\varsigma$.

VI. CONCLUSION

In this paper, we have investigated the optimal EE in two-way OFDM relay system, where the constraints of delay-tolerant QoS and total power consumption are simultaneously considered. We minimize EE by bidirectional bit allocation, which first finds the optimal total bit allocation respectively in two directions by searching the bounds of the feasible region, then assigns the corresponding total bit value on subcarriers using water-filling method. The dimension of the variants optimized is reduced from $2N$ to 1. Simulation results show that our algorithm can on average provide nearly 200% radio energy efficiency performance enhancement than the one without EE optimization. The EE changes when the bounds of feasible region are varied through the number of subcarrier. We also show that as the performance of EE increases when SE decreases, one should make a balance between two factors, which is the subject of future investigations.

ACKNOWLEDGMENT

The authors would like to thank the anonymous referees for their detailed comments on earlier versions of this paper. This work is supported in part by the Key Laboratory of Specialty Fiber Optics and Optical Access Networks, Shanghai University, SKLSFO2012-04, and in part by Shanghai Science Committee under Grant 14511105602 and 14511105902.

APPENDIX A

PROOF OF WATER-FILLING ASSIGNMENT FOR PROBLEM 2

From the constraints of problem 2, we can see that the minimum η_{EE} is obtained when $P_T(\mathbf{B}_{ab}, \mathbf{B}_{ba})$ achieves its minimum value. Observe the expression of $P_T(\mathbf{B}_{ab}, \mathbf{B}_{ba})$ from (5) and the constrains (8a) and (8b), we find that the first term in $P_T(\mathbf{B}_{ab}, \mathbf{B}_{ba})$ is associated with B_{ab}^i but not with B_{ba}^i, while the second term is a function of B_{ba}^i but not of B_{ab}^i, besides, all the constrains on B_{ab}^i and B_{ba}^i are independent. Therefore, problem 2 can be decomposed into two sub-problems respectively for B_{ab}^i and B_{ba}^i with similar form. Take the optimization problem for B_{ab}^i as an example, which is

$$\min_{B_{ab}^i} \sum_{i=1}^{N} \frac{N_0 (2^{\frac{B_{ab}^i}{TW/N}} - 1)}{2|h_{eff}^i|^2}, \tag{20a}$$

$$s.t. \ \sum_{i=1}^{N} B_{ab}^i = B_{ab}, B_{ab}^i \geq 0. \tag{20b}$$

The optimal problem is a convex optimization [34], the Lagrangian function of (20) is given by

$$L(\mathbf{B_{ab}}, \boldsymbol{\lambda}, \mu_1) = \sum_{i=1}^{N} \frac{N_0 (2^{\frac{B_{ab}^i}{TW/N}} - 1)}{2|h_{eff}^i|^2} - \sum_{i=1}^{N} \lambda_i B_{ab}^i - \mu_1 (\sum_{i=1}^{N} B_{ab}^i - B_{ab}),$$

where $\boldsymbol{\lambda} = (\lambda_1, \lambda_2, \cdots \lambda_N)$. μ_1 and $\lambda_i, i = 1, \cdots, N$ are Lagrangian multipliers. The Karush-Khun-Tucker (KKT) conditions are given as

$$\begin{cases} \nabla_{\mathbf{B_{ab}}} L = 0, & (21a) \\ \lambda_i B_{ab}^i = 0, & (21b) \\ \sum_{i=1}^{N} B_{ab}^i = B_{ab}, & (21c) \\ \lambda_i \geq 0, & (21e) \\ B_{ab}^i \geq 0, & (21f) \end{cases}$$

from (21a)，we can get

$$\frac{\partial L}{\partial B_{ab}^i} = \frac{N_0 N \ln 2}{2TW \ |h_{eff}^i|^2} 2^{\frac{B_{ab}^i}{TW/N}} - \lambda_i - \mu_1 = 0, i = 1, \cdots, N, \quad ($$

therefore, we get

$$\lambda_i = \frac{N_0 N \ln 2}{2TW \ |h_{eff}^i|^2} 2^{\frac{B_{ab}^i}{TW/N}} - \mu_1, \quad (2$$

substitute (23) into (21b), we have

$$(\frac{N_0 N \ln 2}{2TW \ |h_{eff}^i|^2} 2^{\frac{B_{ab}^i}{TW/N}} - \mu_1) B_{ab}^i = 0, \tag{24}$$

observe (24), together with (21e) and (21f), we can get

$$B_{ab}^{i}=\max(\frac{TW}{N}\log_2\frac{2TW\,|h_{eff}^{i}|^2}{N_0N\ln 2}\mu_1,0),\tag{25}$$

substitute (25) into (21c), we can get the value of μ_1. Therefore, the water-filling assignment for problem 2 is proved.

APPENDIX B
PROOF OF THEOREM 1

Let $A=TW$, $B=\frac{2TW}{N_0N\ln 2}(|h_{eff}^{1}\cdots h_{eff}^{N}|^2)^{\frac{1}{N}}$. From (13a) and (13b), we get

$$B_{ab}=A\log_2 B\mu_1,\tag{26a}$$

$$B_{ba}=A\log_2 B\mu_2,\tag{26b}$$

substitute (26a) and (26b) into (16), we get

$$\eta_{EE}=2T\frac{\frac{TW}{\ln 2}(\mu_1+\mu_2)-N_0\sum_{i=1}^{N}\frac{1}{|h_{eff}^{i}|^2}}{A\log_2 B\mu_1+A\log_2 B\mu_2}.\tag{27}$$

Suppose the optimal feasible point $D=(\mu_1^*,\mu_2^*)$ of problem 3 is the interior point of the feasible region, then the following equations must establish [34]

$$\left.\frac{\partial\eta_{EE}}{\partial\mu_1}\right|_{\mu_1=\mu_1^*,\mu_2=\mu_2^*}=\left.\frac{\partial\eta_{EE}}{\partial\mu_2}\right|_{\mu_1=\mu_1^*,\mu_2=\mu_2^*}=0.\tag{28}$$

We have

$$\frac{\partial\eta_{EE}}{\partial\mu_i}=2T\left[\frac{\frac{ATW}{\ln 2}\log_2 B^2\mu_1\mu_2}{(A\log_2 B^2\mu_1\mu_2)^2}-\frac{\frac{A\log_2 e}{\mu_i}(\frac{TW}{\ln 2}(\mu_1+\mu_2)-N_0\sum_{i=1}^{N}\frac{1}{|h_{eff}^{i}|^2})}{(A\log_2 B^2\mu_1\mu_2)^2}\right],i=1,2.\tag{29}$$

Substitute (29) into (28), after some arrangements, we get

$$(\frac{1}{\mu_1^*}-\frac{1}{\mu_2^*})(\frac{TW}{\ln 2}(\mu_1^*+\mu_2^*)-N_0\sum_{i=1}^{N}\frac{1}{|h_{eff}^{i}|^2})=0,\tag{30}$$

we can easily prove that the second term of the left side of the equation above can not be zero under the conditions of (12a) and (12b) unless all the channel coefficients are the same, therefore we get $\mu_1^*=\mu_2^*\triangleq\mu^*$. Substitute it into (28), along with (29), we get

$$TW\mu^*\log_2(B\mu^*)^2=\frac{2TW}{\ln 2}\mu^*-N_0\sum_{i=1}^{N}\frac{1}{|h_{eff}^{i}|^2},\tag{31}$$

we can prove that the equation (31) has no solution. A brief interpretation is followed.

Note that the right side of (31) is a linear function $f(\mu^*)$, whose slope is $k_1=\frac{2TW}{\ln 2}$, also note that this line passes through point $E(0,-N_0\sum_{i=1}^{N}\frac{1}{|h_{eff}^{i}|^2})$. The left side of equation (31) is another function

$g(\mu^*)$. Assume that a line l is tangent with $g(\mu^*)$ and passes through point E, after some calculations, we can get that the slope of l is

$$k_2 = TW\log_2[e(|h_{eff}^1 \cdots h_{eff}^N|^2)^{\frac{1}{N}}(\sum_{i=1}^{N}\frac{1}{|h_{eff}^i|^2})]^2,$$

we can prove that $k_2 > k_1$, because the geometric mean is bigger than the harmonic mean, that is to say

$$(|h_{eff}^1 \cdots h_{eff}^N|^2)^{\frac{1}{N}} > \frac{N}{\sum_{i=1}^{N}\frac{1}{|h_{eff}^i|^2}},$$

when $k_2 > k_1$, it can be proved that $f(\mu^*)$ and $g(\mu^*)$ have no intersection point, which can be showed through the following graphic illustration.

The graphics for $f(\mu^*)$ and $g(\mu^*)$ are showed below:

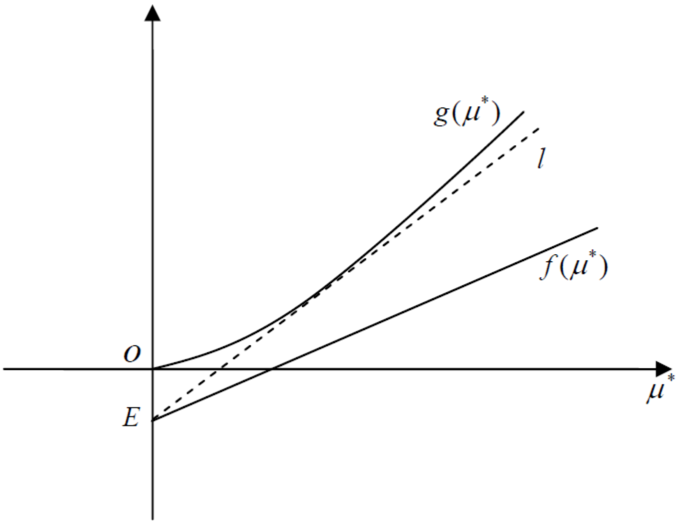

Fig. 9 The illustration for $f(\mu^*)$ and $g(\mu^*)$

Based on (12a), (12b) and the definition of B, we can prove that $B\mu^* \geq 1$, so $g(\mu^*) \geq 0$. The images of $f(\mu^*)$, $g(\mu^*)$ and l are showed in Fig. 9, because $k_2 > k_1$, $f(\mu^*)$ and $g(\mu^*)$ have no intersection point, thus equation (31) has no solution. Theorem 1 is proved.

Competing interests

The authors declare that there is no conflict of interest regarding the publication of this article.

REFERENCE

[1] E. Shih, S. H. Cho, N. Ickes, R. Min, A. Sinha, A. Wang, and A. Chandrakasan, “Physical layer driven protocol and algorithm design for energy-efficient wireless sensor networks,” in ACM MobiCom’01, July 2001.

[2] C. Isheden and G. P. Fettweis, “Energy-efficient multi-carrier link adaptation with sum rate-dependent circuit power,” in Proc. 2010 IEEE Globecom.

[3] T. Wang, and L. Vandendorpe, “On the optimum energy efficiency for flat-fading channels with rate-dependent circuit power,” IEEE Trans. Commun., vol. 61, no. 12, pp. 4910-4921, Dec. 2013.

[4] G. Miao, N. Himayat, and G. Y. Li, “Energy-efficient link adaptation in frequency-selective channels,” IEEE Trans. Commun., vol. 58, no. 2, pp. 545-554, Feb. 2010.

[5] C. Sun, Y. Cen, and C. Yang, “Energy efficient OFDM relay systems,” IEEE Trans. Commun., vol. 61, no. 5, pp.1797-1809, May 2013.

[6] R. Pabst, B. H. Walke, D. C. Schultz, P. Herhold, H. Yanikomeroglu, S. Mukherjee, H. Viswanathan, M. Lott, W. Zirwas, M. Dohler, H. Aghvami, D. D. Falconer, and G. P. Fettweis, “Relay-based deployment concepts for wireless and mobile broadband radio,” IEEE Commun. Mag., vol. 42, no. 9, pp. 80-89, Sep. 2004.

[7] J. Ping and S. H. Ting, “Rate performance of AF two-way relaying in low SNR region,” IEEE Commun. Letters, vol. 13, no.

4, pp. 233-235, Apr. 2009.
[8] J. Yang, P. Fan, T. Q. Duong, and X. Lei, “Exact performance of two-way AF relaying in Nakagami-m fading environment,” IEEE Trans. Wireless Commun., vol. 10, no. 3, pp. 980-987, Mar. 2011.
[9] I. Krikidis, “Relay selection for two-way relay channels with MABC DF: A Diversity Perspective,” IEEE Trans. Veh. Technol., vol. 59, no. 9, pp. 4620-4628, Nov. 2010.
[10] Y. Yang, and S. Aissa, “Information-guided transmission in decode-and-forward relaying systems: spatial exploitation and throughput enhancement,” IEEE Trans. Wireless Commun., vol. 10, no. 7, pp. 2341-2351, July 2011.
[11] S. Zhang, S. C. Liew, P. P. Lam, “Physical-layer network coding,” in ACM MobiCom’06, Sep. 2006.
[12] S. Katti, H. Rahul, W. Hu, D. Katabi, M. Médard, and J. Crowcroft, “XORs in the air: Practical wireless network coding,” IEEE/ACM Trans. Netw., vol. 16, no. 3, pp. 497-510, Jun. 2008.
[13] V. T. Muralidharan, and B. S. Rajan, “Performance analysis of adaptive physical layer network coding for wireless two-way relaying,” IEEE Trans. Wireless Commun., vol. 12, no.3, pp. 1328-1339, Mar. 2013.
[14] B. Nazer, and M. Gastpar, “Reliable physical layer network coding,” Proc. IEEE, vol.99, no.3, pp. 438-460, Mar. 2011.
[15] S. Zhang, S. C. Liew, and P. P. Lam, “On the synchronization of physical-layer network coding,” in Proc. IEEE Inf. Theory Workshop, Chengdu, China, Oct. 2006, pp. 404-408.
[16] C. K. Ho, R. Zhang, and Y. C. Liang, “Two-way relaying over OFDM: optimized tone permutation and power allocation,” in Proc. 2008 IEEE ICC.
[17] W. Dang, M. Tao, H. Mu and J. Huang, “Subcarrier-pair based resource allocation for cooperative multi-relay OFDM systems,” IEEE Trans. Wireless Commun., vol. 9, no.5, pp. 1640-1649, May 2010.
[18] S. Shahbazpanahi and M. Dong, “Achievable rate region and sum-rate maximization for network beamforming for bi-directional relay networks, ” in Proc. 2010 IEEE ICASSP.
[19] C. Xiong, G. Y. Li, S. Zhang, Y. Chen, and S. Xu, “Energy-and spectral-efficiency tradeoff in downlink OFDMA networks,” IEEE Trans. Wireless Commun., vol. 10, no. 11, pp. 3874-3886, Nov. 2011.
[20] C. Xiong, G. Y. Li, S. Zhang, Y. Chen, and S. Xu, “Energy-efficient resource allocation in OFDMA networks,” IEEE Trans. Commun., vol. 60, no. 12, pp. 3767-3778, Dec. 2012.
[21] W. Guo and T. O’Farrell, “Relay deployment in cellular networks: planning and optimization,” IEEE J. Sel. Areas Commun., vol. 31, no. 8, pp. 1597-1606, Aug. 2013.
[22] J. Qu, Y. Cai, and W. Yang, “Energy-efficient joint resource allocation in two-way OFDM relay system,” in IEEE ICIST, Yangzhou, Jiangsu, China, pp. 1237-1241, Mar. 2013.
[23] X. Wang, G. B. Giannakis, and A. G. Marques, “A unified approach to QoS-guaranteed scheduling for channel-adaptive wireless networks,” Proc. IEEE, vol. 95, no.12, pp. 2410-2431, Dec. 2007.
[24] S. Kim and Y. H. Lee, “Energy-efficient power allocation for OFDM signaling over a two-way AF relay,” IEEE Trans. Veh. Technol., vol. 64, no. 10, pp. 4856-4863, Oct. 2015.
[25] C. Xiong, L. Lu and G. Y. Li, “Energy-efficient OFDMA-based two-way relay,” IEEE Trans. Commun., vol. 63, no. 9, pp. 3157-3169, Sep. 2015.
[26] E. Bedeer, A. Alorainy, M. J. Hossain, O. Amin, and M. S. Alouini, “Fairness-aware energy-efficient resource allocation for AF co-operative OFDMA networks,” IEEE J. Sel. Areas Commun., vol. 33, no. 12, pp. 2478-2493, Dec. 2015.
[27] W. Guo, S. Wang, C. Turyagyenda, and T. O’Farrell, “Integrated cross-layer energy savings in a smart and flexible cellular network,”in Proc. 2012 IEEE ICCC.
[28] S. Cui, A. J. Goldsmith, and A. Bahai, “Energy-constrained modulation optimization,” IEEE Trans. Wireless Commun., vol. 4, no. 5, pp. 2349-2360, Sep. 2005.
[29] C. Sun and C. Yang, “Energy efficiency analysis of one-way and two-way relay systems,” EURASIP J. Wireless Commun. and Networking, vol. 2012, no. 46, pp. 1-18, Feb. 2012.
[30] H. A. Suraweera, P. J. Smith, A. Nallanathan, and J. S. Thompson, “Amplify-and-Forward relaying with optimal and suboptimal transmit antenna selection,” IEEE Trans. Wireless Commun., vol. 10, no. 6, pp. 1874-1885, June 2011.
[31] Q. Jiang, H. Chen, and X. Liao, “Joint power allocation and subcarrier assignment for two-way OFDM multi-relay system,” in Proc. 2013 IEEE WCNC.
[32] F. He, Y. Sun, L. Xiao, X. Chen, C. Y. Chi, and S. Zhou, “Capacity region bounds and resource allocation for two-way OFDM relay channels,” IEEE Trans. Wireless Commun., vol. 12, no. 6, pp. 2904-2917, June 2013.
[33] Y. Ma, N. Yi and R. Tafazolli, “Bit and power loading for OFDM-based three-node relaying communications,” IEEE Trans. Signal Process., vol. 56, no. 7, pp. 3236-3247, July 2008.
[34] S. Boyd and L. Vandenberghe, Convex Optimization. Cambridge University Press, 2004.
[35] Q. Cui, T. Yuan, X. Tao, A. A. Dowhuszko, and R. Jäntti, “Energy efficiency analysis of two-way DF relay system with non-ideal power amplifiers,” IEEE Commun. Lett., vol. 18, no. 7, pp. 1254-1257, July 2014.
[36] H. Yu, Y. Li, X. Zhong, L. Wang, and J. Wang, “The analysis of the energy efficiency for the decode-and-forward two-way relay networks,” in Proc. 2013 IEEE WCNC: PHY.
[37] S. Verdu, “Spectral efficiency in the wideband regime,” IEEE Trans. Inf. Theory, vol. 48, no. 6, pp. 1319-1343, June 2002.